 DOI: 10.1002/mawe.200500968

Biocompatibility of ceramic scaffolds for bone replacement made by 3D printing

Biokompatibilität 3D gedruckter keramischer Scaffolds als Knochenersatz

B. Leukers[1], H. Gülkan[2], S. H. Irsen[1], S. Milz[3], C. Tille[1], H. Seitz[1], M. Schieker[2]

Bone replacement materials used in tissue engineering require a high degree of safety and biological compatibility. For these reasons synthetic bone replacement materials based on calcium-phosphates are being used more widely. To mimic natural bone, rapid prototyping processes and especially 3D printing are favourable. Using 3D printing, complex 3 dimensional structures can be made easily.

In this study we successfully performed biocompatibility tests with a Hydroxyapatite test structure (HA-S) made by 3D printing. Cytotoxicity tests were carried out according to DIN ISO 10993-5 in static and dynamic cultivation setups. To estimate cell proliferation and analyze morphology, histological evaluation was done. In summary, good cell viability as well as good proliferation behaviour were found. Moreover, these results show that the 3D printing process in combination with the suitable material presented in this study is well suited for fabricating scaffolds for TE in the required accuracy and biological compatibility.

Key words: Scaffold fabrication, cell culture, biocompatibility, hydroxyapatite, 3D printing

Knochenersatzmaterialien für das Tissue Engineering (TE) erfordern ein hohes Maß an Sicherheit und biologischer Verträglichkeit. Aus diesen Gründen nehmen synthetische Knochenersatzmaterialien auf der Basis von Calciumphosphaten einen immer größer werdenden Stellenwert ein. Um der Struktur des natürlichen Knochens so nahe wie möglich zu kommen, bieten sich Verfahren aus dem Rapid Prototyping, insbesondere das 3D Drucken an. Dadurch lassen sich komplexe, dreidimensionale Strukturen für das TE einfach herstellen.

In dieser Studie haben wir erfolgreich eine mittels 3D Drucken hergestellte Struktur (HA-S) auf der Basis von Hydroxylapatit auf ihre Biokompatibilität getestet. Zytotoxizitätsuntersuchungen wurden analog DIN ISO 10993-5 in statischer und dynamischer Kultivierung durchgeführt. Zudem wurden histologische Schnitte zur Beurteilung der Zellproliferation und -morphologie durchgeführt. Insgesamt konnte eine gute Zellvitalität und Zellproliferation nachgewiesen werden. Darüber hinaus zeigen die Ergebnisse, dass das hier vorgestellte 3D Druckverfahren mit dem hier verwendeten Material dazu geeignet ist, Strukturen für das TE in ausreichender Präzision und biologischer Verträglichkeit herzustellen.

Schlüsselworte: Scaffoldherstellung, Zellkultur, Biokompatibilität, Hydroxylapatit, 3D Drucken

1 Introduction

Bone grafts have been used for a long time to repair osseous defects from trauma or disease. While autografts are limited in availability and are difficult to shape, allo- or xenografts require extensive processing to minimize disease transmission. In contrast, synthetic bone replacement materials are safe in use and easy to obtain. Today, various synthetic bone replacement materials based on Calciumphosphates are available [1]. Normally these materials are available as granulates or produced in simple geometries such as blocks, pins or splines with drilled holes for medium supply.

To ensure good vascularisation of the scaffolds and good attachment of bone cells, and to guide their growth in all dimensions, interconnective pores with diameters of about 500 μm are discussed in literature as to be favored [2].

The use of rapid prototyping (RP), also known as solid freeform fabrication technology, allows the production of scaffolds with defined and reproducible internal structures taken straight from computer data [3]. Each RP process has advantages and disadvantages in fabricating 3D scaffolds. In literature, two different methods to generate scaffolds using RP are described [4–11]. On the one hand, custom implants can be fabricated directly from computer data to produce a complex geometry using the desired material. On the other hand, there are indirect methods where a negative mold as template for the interconnective network of pores is fabricated via RP technology. The negative is casted with the desired material. After casting, the template can be removed by pyrolysis, dissolving or melting.

For generating e.g. Hydroxyapatite (HA) or β-Tricalciumphosphate (β-TCP) -based scaffolds for bone replacement, RP techniques such as stereolithography or a dispensing system are described in literature [4–6]. Most of these techniques for scaffold fabrication use the indirect method. For example, negative molds based on photocurable epoxy resins are created using stereolithography. Then they are casted with a slurry consisting of hydroxyapatite and a binder compound. The negative mold is pyrolysed in a sinter furnace. The HA positive remains in the sinter furnace for consolidation [4]. Another indirect fabrication method uses a dispense technique: thermoplastics are used as negative mold material that can be melted at low temperature and so avoids sintering [5].

For direct fabrication of three-dimensional networks a dispensing method using a chitosan-HA formulation has been reported [6].

[1] Research center caesar, Bonn

[2] Experimental Surgery and Regenerative Medicine, Department of Surgery – Downtown, University of Munich, München

[3] Anatomische Anstalt, Ludwig-Maximilians-Universität München, München

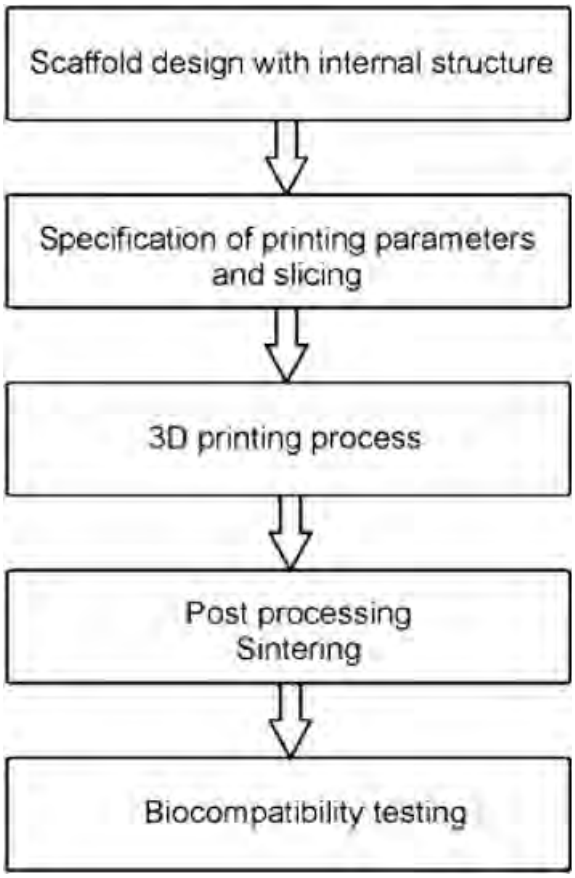

Figure 1. Flow chart of HA-scaffold design used for biocompatibility testing.

Abbildung 1. Flussdiagramm des Prozessablaufs vom Scaffolddesign zur Biokompatibilitätsprüfung.

Another direct RP technique for scaffold design is the 3D printing process [12]. To achieve a powder-based manufacturing process, a computer model provides defined layers, which are printed with a suitable binder onto a powder bed. The wetted regions harden and the result of this layer-based printing process is a 3D copy of the computer model. A main advantage of 3D printing is the great choice of materials. It is a promising method for direct fabrication of custom implants. Besides the possibility to control the structure of inner channels, the outer shape of the scaffold can be designed based on a patient's computer tomography data to design an individual implant for a given bone defect.

In literature, 3D printing is discribed for creating resorbable scaffolds based on poly(lactic acid) [7,8] or poly(lactic-co-glycolic acid) [9] powder and ceramics[10]. Another author used starch-based polymer powder [11].

Our goal is the direct fabrication of ceramic scaffolds for bone tissue engineering using a 3D printing process. We use HA powder to fabricate porous ceramic structures with designed internal architecture. HA is a promising bone replacement material because of its stoichiometric similarity to the inorganic part of natural bone. We optimized the printing process to fabricate high resolution interconnective structures with channel diameters of less then 500 μm and a wall thickness of approximately 330 μm. The whole process was published recently by our group [13].

Because the ceramic structures will be used as scaffolds for bone implants, it is important to investigate their biocompatibility as well as ingrowth of cells into the 3D structure. Therefore, we developed a test structure (named HA-S) with a specific design and defined internal structure for biocompatibility tests in this study. The objective of the design was to maximize the surface, to facilitate the seeding process for enhanced cell adhesion, and to enable a good supply of the interior of the scaffold with medium.

To ensure biocompatibility of the ceramic structure, cell viability and cell morphology were investigated in static and dynamic cultivation setups. Viability of cells was tested using a colorimetric assay based on the reduction of a tetrazolium salt [14, 15]. Additionally, histological evaluation was carried out. Cell adhesion on the designed internal structure, cell ingrowth into the bulk material and cell morphology were analyzed.

A flow chart of the process starting with scaffold design to biocompatibility testing is shown in *Figure 1*.

2 Material and Methods

2.1 Materials

In this study we used a spraydried HA-granulate named V5. Besides the main component HA, it contains polymeric additives to improve bonding and flowability. As a binder, we used Schelofix which consists of water soluble polymeric compounds. Materials were obtained from the Friedrich-Baur-Institute (FBI, Bayreuth, Germany). For printing, the binder powder was dissolved in water to yield a 14 % solution (w/w).

2.2 Scaffold design

The design of the test structure for biocompatibility testing was done by RP software Magics 9.14 (Materialise, Leuven, Belgium).

The resulting Computer Added Design (CAD) test structure HA-S was cylindrically shaped with a height of 7 mm and 12 mm in diameter, designed to fit into a 48 well plate cavity as well as into a perfusion chamber (MINUCELLS and MINUTISSUE GmbH, Bad Abbach, Germany) after shrinking during the sintering process. *Figure 2a* shows the whole structure in front view and *Figure 2b* presents a horizontal clip-plane view of the structure. The internal architecture of the specimens was made of parallel walls all of which stand in angles of 45° to the x-axis. The walls were held together by a parting plane rotated by 90° about the z-axis relative to the other walls with a tilt angle of 45° to the y-axis. To improve the stability of the HA-S the walls were held together on top by a semi-circular structure. The distance between vertical walls was 1.2 mm, wall thickness was about 1.0 mm and the overall surface was 1040 mm^2.

2.3 Data preparation

The CAD model (.stl format) was sliced into 300 μm horizontal layers by a slicing algorithm using the software Magics 9.14 (Materialise, Leuven, Belgium). Thereby, the data were converted into .slc (SliCe) format. Ctools, a module of Magics, was used to set the printing resolution in x- (0.2 mm) and y-direction (0.2 mm). After defining the voxelsize, the data were converted into bitmap files. The 2 dimen-

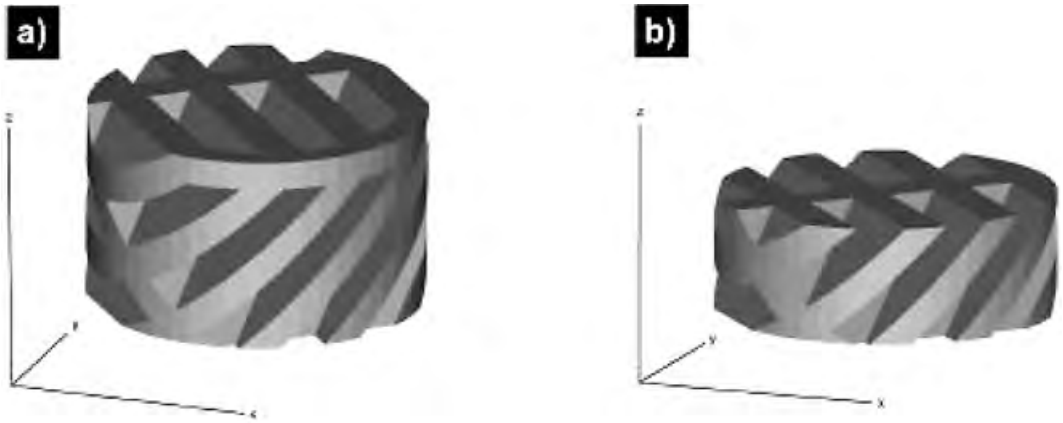

Figure 2a. Front view of designed CAD test structure for biocompatibility testing. **2b)** horizontal clip-plane view.
Abbildung 2a. Vorderansicht der CAD Teststruktur zur Biokompatibilitätsprüfung. **2b)** Ansicht horizontale Schnittfläche.

sional bitmap files were imported into the print control software.

2.4 3D printing and post processing

In this study we used a 3D printing test setup which we developed in cooperation with Generis GmbH (Augsburg, Germany). The flexibility of this test setup makes it possible to investigate new process techniques as well as new material combinations. The sliced layers were built up by the printer setup to create the three dimensional HA-S layer by layer. After printing each layer the platform was lowered according to the layer thickness of 300 μm and a new layer of ceramic powder was deposited onto the former one. After finishing, slight air flow was used to remove unbound powder trapped in internal structures of the HA-S. To receive sufficient strength of the test bodies and to remove the organic binder compound, specimens were sintered for two hours at 1300 °C in a high temperature furnace (Carbolite GmbH, Ulbstadt-Weiher, Germany). The size of the HA-S was about 9,5 mm in diameter and 5,5 mm in height. The shrinkage of the HA-S was approximately 18 – 20 % in all directions.

2.5 SEM analysis

SEM analysis was performed on LEO supra 55 SEM (Carl Zeiss SMT AG, Oberkochen, Germany). The scaffolds – one of them was embedded in poly(urethane) - were sputtered with a gold layer of approximately 18 nm (MED 20, BAL-TEC AG, Balzers, Liechtenstein). Scaffolds were examined under high vacuum conditions at 10 kV.

2.6 Cell culture

MC3T3-E1 osteoblast-like cells were obtained from DSZM (Braunschweig, Germany). Cells were cultured in α-MEM (Gibco® Invitrogen Cell Culture, Karlsruhe, Germany) supplemented with ribonucleosides, deoxyribonucleosides and 2 mM GlutaMAX^{TM}I manufactured containing 10 % (v/v) heat-inactivated fetal calf serum (Sigma, Munich, Germany), 40 IU/ml penicillin (Gibco® Invitrogen Cell Culture, Karlsruhe, Germany) and 40 μg/ml streptomycin (Gibco® Invitrogen Cell Culture, Karlsruhe, Germany) in a humidified incubator at 37 °C with 5 % CO_2. The medium was refreshed every 3-4 days and cells were passaged after reaching a confluence of 90 to 100 %.

2.7 Scaffold seeding

Before cell seeding, each steam sterilised HA-S was placed into a 48 well plate cavity (Nunc, Wiesbaden, Germany) and prewetted with cell culture medium for 6 to 8 hours and with heat-inactivated fetal calf serum over night. For cell viability and morphological investigations, the scaffolds were seeded with 5 x 10^4 MC3T3-E1 murine fibroblasts contained in 600 μl suspension per scaffold to enable covering of the scaffolds. Throughout the whole seeding process, the HA-S were incubated at 37 °C with 5 % CO_2. During the first 2 hours, the cell suspension was resuspended every 20 minutes and the HA-S subsequently turned. This procedure was repeated once an hour for the next 2 to 3 hours. The HA-S were incubated for 1 hour and then they were transferred into a new cavity of a 48 well plate for cultivation. Altogether, the process of seeding took 5–6 hours. Seeding efficiency was calculated by counting the number of cells remaining in the 48 well cavity where the seeding was carried out. For static culture each scaffold was cultivated up to 7 days in one cavity of a 48 well plate with 600 μl cultivation medium. The medium was changed twice a week. Dynamic cultivation was performed using a pump with a flow rate of 18 μl/min (Ismatec GmbH, Wertheim-Mondfeld, Germany) in perfusion containers (MINUCELLS and MINUTISSUE GmbH, Bad Abbach, Germany) in a humidified incubator at 37 °C and with 5 % CO_2. On day 1 and day 7 after seeding, HA-S were embedded into methyl methacrylate (MMA) to investigate cell viability and cell morphology.

2.8 Cell viability assay

Cell activity of seeded HA-S was measured by performing a tetrazolium assay (WST-1, Roche, Mannheim, Germany). As control, MC3T3-E1 cells were used. To apply cell numbers comparable to those on HA-S we seeded MC3T3-E1 cells in 12 well plates at a density 4 x 10^4 cells/well depending on a seeding efficiency on HA-S of approximately 82 %.

Non-seeded HA-S and plastic dishes were cultured similarly and served as a blank for seeded HA-S and plastic dishes, respectively. The scaffolds were transferred to new 48 well plate cavities and 600 μl WST-1 reagent 1:10 diluted in medium was added. After 2 hours incubation at 37 °C and 5 % CO_2, two times 100 μl supernatant were transferred from each sample to a 96 well plate. The absorbance was measured at 450 nm using a spectrophotometer (MRX TL, DYNEX Technologies, Virginia, USA). The background (reference wavelength) was determined at 630 nm and was substracted from the absorbance at 450 nm.

2.9 Histological examination

One sample of each group was collected at day 1 and day 7 for histological examination. The specimens were fixed in 100 % methanol, incubated in 50 % methyl metharcylate (MMA) (Merck, Schuchardt OHG, Hohenbrunn, Germany) and 50 % methanol for 3 days, followed by two times 100 % MMA incubation for three days. Then the specimens were incubated in MMA-polymerization medium for three days and finally transferred into air tight glass vials filled with the same MMA-medium. The polymerization was started by rising the temperature to about 27 °C and the blocks were hardened for approx. 7 days. After removal of the glass, the embedded samples were sectioned orthogonal to the flat surface of the scaffolds at 100 $\pm$ 10 μm using a saw microtome SP1600 (Leica, Wetzlar, Germany). Sections were stained with paragon to visualise cells and nuclei. The specimens were mounted on glass slides with EUKIT (O. Kindler GmbH&Co, Freiburg, Germany) and then were examined under a light microscope (Zeiss Axiophot, Carl Zeiss AG, Jena, Germany). Representative images were acquired using a 3-CCD Colour Video Camera (Sony, Köln, Germany) and KS400 software (Carl Zeiss AG, Jena, Germany).

3 Results

3.1 Printing results and SEM analysis

We successfully printed HA-S for the biocompatibility tests. The specimens were stable and trapped HA-powder could be removed easily with slight airflow. No distortion was detectable. *Figure 3* shows the whole HA-S after sintering. To examine the surface structure of the HA-S, SEM analysis was performed. *Figure 4a – c* show a top view of the surface structure of a HA-S. *Figure 4d – f* represent cross-sections in different magnifications to observe inner structures. Figure 4a shows the surface structure of the whole HA-S in 28-fold magnification, while a 65-fold magnification showing an insight of a cavity is provided in Fig. 4b. The geometry of the HA-S is remained after sintering (Figure 4a). Its contours are largely accurate while the granule structure of the HA-powder is still distinguishable (Figure 4b). Figure 4c shows the granule structure in detail with its characteristic microporosity. Over the whole HA-S this porosity is almost homogenous (Figure 4d, 4e). Moreover, there are sinter necks which contribute to mechanical stability (Figure 4f).

Figure 3. Printed test structure HA-S after sintering.
Abbildung 3. 3D gedrucktes Testbauteil HA-S nach dem Sintern.

3.2 Cell viability and histological evaluation

To test for the biocompatibility of a given material in direct contact to tissue, the ISO 10933-5 norm allows for a qualitative assessment of cytotoxicity. Therefore, we analysed cell activity and cell morphology at day 1 and day 7 for two samples.

Seeding efficiency was improved by modifying conventional static cell seeding protocols. Cell suspension was mixed every 20 min for 2 hours. By extending the seeding time to an overall of 5 to 6 hours we obtained seeding efficiencies of approximately 82 %.

The vitality of MC3T3-E1 cells seeded onto HA-S and subsequently cultivated statically or dynamically were studied by the WST-1 viability assay, which allows to correlate an optical signal (absorbance (A450 nm – A630 nm)) with the number of viable cells [16]. *Figure 5* summarizes the cell vitality data of MC3T3-E1 cells on the surfaces of porous HA-S and plastic wells. Absorbance (A450 nm – A630 nm) increased from day 1 to day 7. In contrast to cells on plastic, cells on HA-S exhibited a lower absorbance (A450 nm – A630 nm) at day 1. Within the first week absorbance (A450 nm – A630 nm) showed a five-fold increase for cells cultivated on plastic. Cells cultivated statically or dynamically on HA-S gave rise to a 13-fold and 16-fold stronger absorbance (A450 nm – A630 nm) up to day 7, respectively. Under static culture conditions cell outgrowth from the HA-S to the plastic surface was observed within a few days. These cells adhered to the dish and formed a monolayer culture (not shown).

To further assess cell proliferation and cell growth on HA-S, we performed a histological analysis of slides taken at various depths from the seeded surface at day 1 and day 7. On day 1 of culture, paragon staining revealed the presence of cells spread over the material's surface. At this stage, only single cells were observed under static and dynamic culture conditions, as is shown in *Figure 6a* for static cultivation. After one week in culture, the number of cells attached to the materials surfaces had increased. All test structures were now covered with multiple layers of cells (*Figure 6b*). Cells were present in both the outer and the inner parts of the HA-S as shown in *Figure 6c* and *Figure 6d*, respectively. Both cultivation meth-

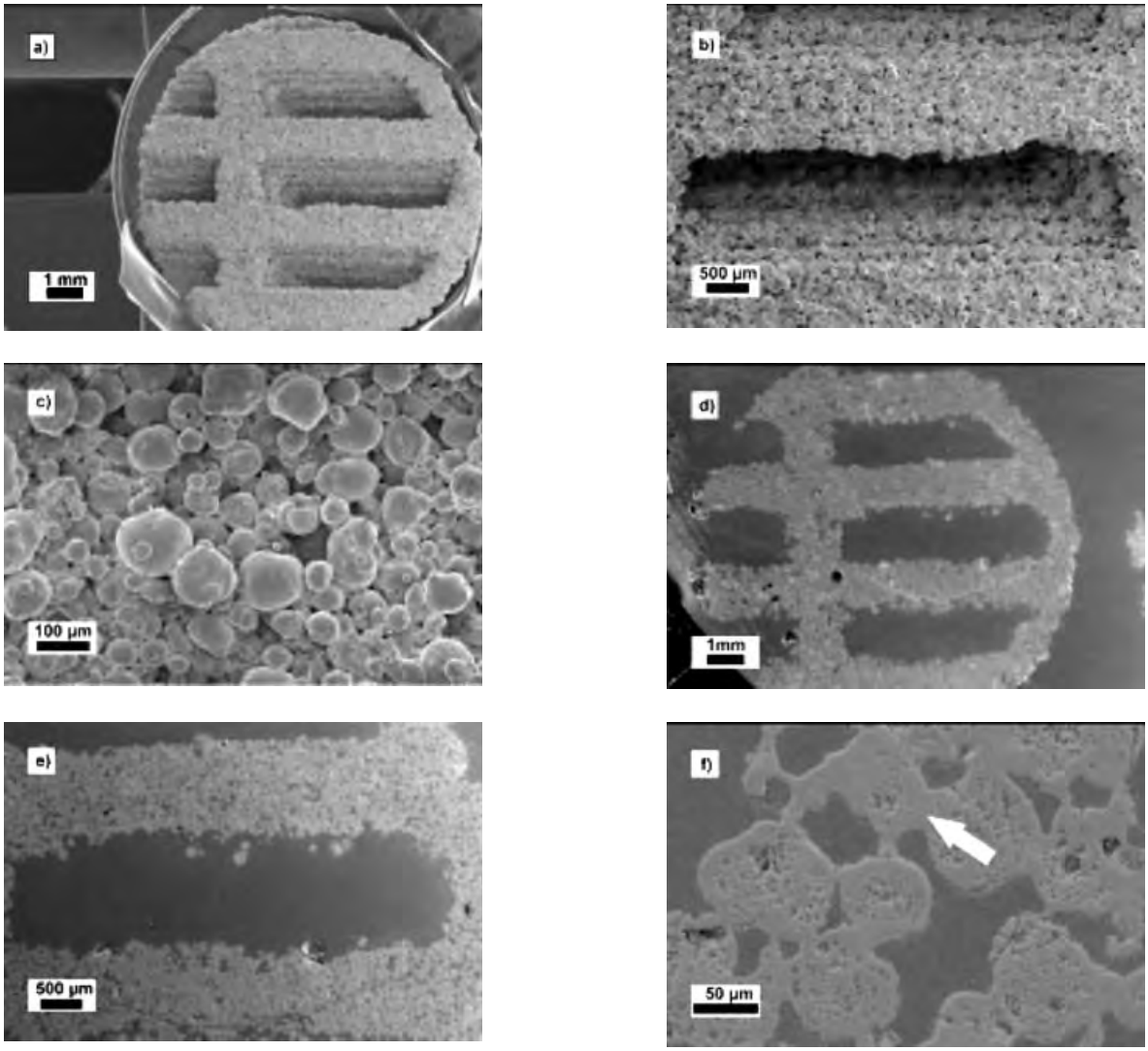

Figure 4a. – c. SEM pictures of surface structure (top view). The granule structure is visible after sintering.
Abbildung 4a. – c. SEM Abbildung der Oberflächenstruktur. Gut zu erkennen ist der Erhalt der Granalienstruktur nach dem Sintern.
Figure 4d. – f. Corresponding SEM cross-sections in top view. Homogenous porosity is detectable. The white arrow shows a sinter neck.
Abbildung 4d. – f. Dazugehörige Schliffbilder in Aufsicht. Eine gleichmäßige Porosität ist erkennbar. Der weiße Pfeil zeigt einen ausgeprägten Sinterhals.

ods were clearly distinguishable with respect to growth behaviour of cells on and into cavities of HA granules: While cells on statically cultured scaffolds formed multiple layers and were located mostly on the surface of the HA-S (Figure 6b), cells on dynamically cultured HA structures tended to grow into cavities of the granules (Figure 6c and Figure 6d).

4 Discussion

In this study, we showed that the V5-hydroxyapatite scaffolds (HA-S) made by 3D printing caused no cytotoxicity after sintering. For the biocompatibility tests we developed a specific test structure with inclined layers of 45° (Figures 2a and 2b) Advantages of this specific structure are facilitation of the seeding process, because cells do not slip off the structure, and proliferation to the inside of the HA-S without clogging. The powder-based 3D printing process enabled us to create structures with a high surface roughness. In literature, the influence of surface roughness on cell attachment and proliferation is described mainly in conjunction with grinded surfaces and is discussed controversial [17]. When trying to relieve cells from our HA-S with Trypsin in preliminary studies, we observed very strong cell attachment. Moreover, we received a good seeding efficiency of the HA-S of about 82 % measured according to our conditions. Therefore we assume, that the remaining of the granule structure in range of less then 100 μm is a promising environment for cell attachment.

The 3D printing process creates a structure with high microporosity. A highly porous structure is important for future application as scaffold material for bone repair because microporosity is supposed to improve the biodegradability [18]. In comparison to dense HA-ceramics, the higher surface of 3D printed HA-S might improve the slow resorption rate of HA. Additionally, the formation of new bone was reported of sin-

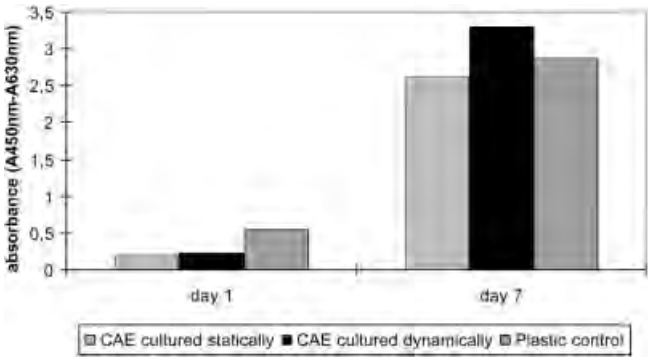

Figure 5. Cell viability analysis of MC3T3-E1 fibroblasts seeded on porous HA scaffolds cultured statically and dynamically. As control the plastic surface of the microtiter plate was used. WST-1 assay were performed on day 1 and day 7. OD 450 value was averaged from two experiments.

Abbildung 5. Zellvitalitätssassay: MC3T3-E1 Fibroblasten wurden auf die porösen HA Scaffolds ausgesät und diese unter statischen und dynamischen Bedingungen kultiviert. Als Kontrolle diente die besiedelte Plastikoberfläche der Mikrotiterplatte. Die Zellvitalität wurde an Tag 1 und Tag 7 der Kultivierung bestimmt. Es wurde der Mittelwert aus zwei Versuchen gebildet.

tered 3D printed HA-scaffolds implanted into a rabbit. They observed unusually amounts of new bone in pores smaller than 20 μm [10].

Examining the cell viability we observed clear differences between cells on HA-S and control dishes on day 1. Stress e.g. due to the seeding procedure one day before, could have caused a lowered absorbance (A450 nm – A630 nm) compared to cells seeded conventionally due to the fact that stress seems to reduce WST-1 reduction [19]. Alternatively different seeding conditions and/or growth conditions could change oxygen supply resulting in an altered amount of superoxide which is generated by oxygen reduction and which is responsible for WST-1 reduction [20, 21, 22]. Another reason might be that a major part of cells attached on the HA surface have died [23]. On day 7, cells seeded on HA-S and cultured dynamically showed a higher cell activity than statically cultured cells either on plastic or on HA structures. A dynamic cell culture system seems to allow for an adequate supply of nutrients, resulting in higher cell activity or cell proliferation compared to statically cultured cells [24]. It is important to point out that the results of the WST-1 assay do not allow quantification of cell number; the results only allow for a relative comparison of overall metabolic activity. The assay is, however, useful to compare different experimental conditions in a three-dimensional construct.

The histological examination allows for evaluation of local cell distribution, morphology and proliferation within different regions of the HA scaffolds.

Paragon staining after 7 days in culture verified that cells populated the outer and inner surface of HA-S, thus forming a continuous layer which delineates the scaffold contour. Dynamic cell culture led to a large number of cells growing into the cavities between HA granules. This type of growth was different from that of statically cultured cells. The perfusion cell system seems to facilitate the supply with nutrients

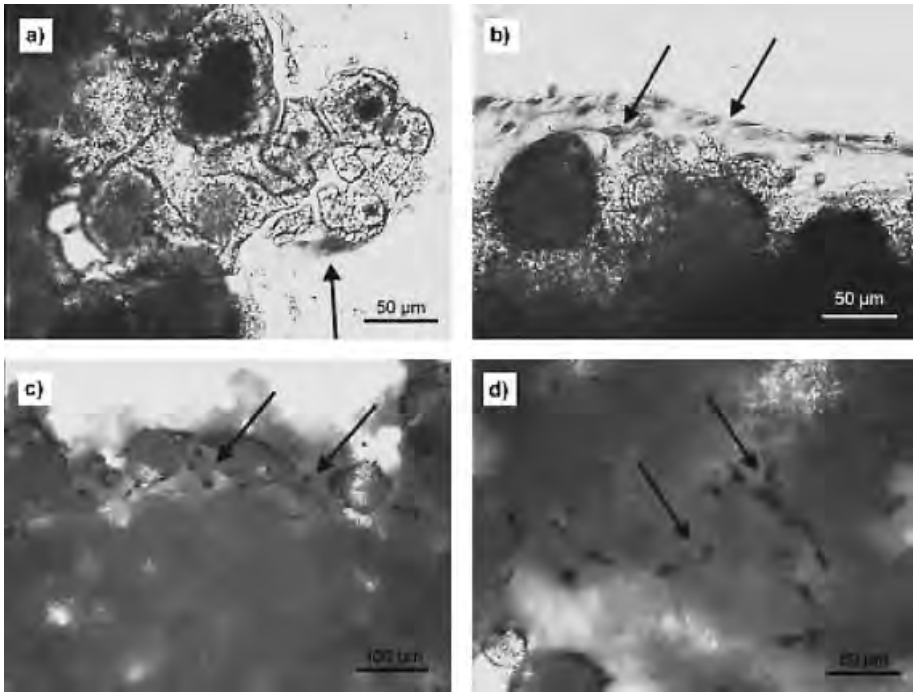

Figure 6. Paragon-stained cross-sections of HA scaffolds seeded with MC3T3-E1 cells and cultured statically or dynamically up to 7 days. The grey area represents HA ceramic. Paragon-stained cells (cytoplasm and cell nuclei) are marked in a) and b) by arrows pointing to a single cell or cell layer, respectively. In c) and d) paragon stained cells are clearly darker than surrounding HA ceramic. a: statically cultured for one day. b: statically cultured for 7 days. c: dynamically cultured for 7 days (outer part). d: dynamically cultured for 7 days (inner part).

Abbildung 6. Mittels Paragon gefärbte Schnittbilder der HA-Scaffolds. Die Scaffolds wurden statisch und dynamisch bis zu 7 Tagen kultiviert. Die grauen Bereiche zeigen die HA-Keramik. Mit Paragon gefärbte Zellen (Zellkerne und Zytoplasma) sind in Abbildung a) und b) mit Pfeilen markiert, die einzelne Zellen (a) oder Zelllayer (b) zeigen. In Abbildung c) und d) sind die Zellen deutlich dunkler als die umliegende HA- Keramik. a: Statische Kultivierung 1 Tag. b: Statische Kultivierung 7 Tage. c: Dynamische Kultivierung 7 Tage (äußerer Bereich). d: Dynamische Kultivierung 7 Tage (innerer Bereich).

and oxygen leading to better ingrowth of cells into the scaffolds' cavities. An alternative explanation might be that cells on HA-S have grown deeply into the cavities between HA granules to take shelter from the fluid shear forces caused by a flow rate of 18μl/min [25].

Both approaches demonstrate that cells maintain their morphology, attach well to and proliferate on HA-S. These findings are important for further engineering of bone grafts, because growth and differentiation capabilities of cells seeded onto HA-S should be retained for a certain period of culture in order to achieve a better outcome.

5 Conclusions

In this study we designed a special HA-S for biocompatibility tests. Cells cultured on these structures showed good viability. Furthermore, especially in dynamic cultivation, the cells colonized inner portions of the test structure whilst retaining their morphology.

These results are of relevance for future application of HA-S in bone tissue engineering. It is obvious that this material does not exert any cytotoxicity after sintering and that adhering cells proliferate adequately. The flexibility of the 3D printing process offers the possibility to realize more complex structures than described in this paper. By now we have modified the presented test structure design and asses osteogenic differentiation in 3D culture. This advanced structure has more than one parting wall to create more channel-like structures as it is required for bone tissue engineering.

Together, the results of this study are important for future applications of sintered HA-S as scaffold material for bone replacement. Hence, the 3D printing process based on HA powder is promising for producing patient-specific implants for bone repair with interconnective 3D structures.

6 Acknowledgements

This work was supported by ForTePro (Bayerischer Forschungsverbund für Tissue Engineering und Rapid Prototyping) funded by the Bayerische Forschungsstiftung. We would like to thank Frau B. Hackl and Frau C. Harbauer for their excellent technical assistance.

7 References

1. D. Tadic, M. Epple, *Biomaterials* **2003**, *25*, 987.
2. O. Gauthier, J. M. Bouler, E. Aguado, P. Pilet, G. Daculsi, *Biomaterials* **1998,** *19*, 133.
3. S. Yang, K. F. Leong, Z. H. Du, C. H. Chua, *Tissue Engineering* **2002**, *8(1)*, 1.
4. T. M Chu, D. G. Orton, S. J. Hollister, S. E. Feinberg, J. W. Halloran, *Biomaterials* **2002**, *23*, 1283.
5. E. Charrière, J. Lemaitre, Ph. Zysset, *Biomaterials* **2003**, *24*, 809.
6. T. H. Ang, F. S. A. Sultana, D. W. Hutmacher, Y. S. Wong, J. Y. H. Fuh, X. M. Mo, H. T. Loh, E. Burdet, S. H. Teoh, *Materials Science and Engineering* **2002**, *C 20*, 35.
7. R. A. Giordani, B. M. Wu, S. W. Borland, L. G. Cima, E. M. Sachs, M. J. Cima, *J Biomater Sci Polym Edn* **1996**, *8 (1)*, 63.
8. A. Park, B. Wu, L. G. Griffith, *J Biomed Sci Polym Edn* **1998**, *9*, 89.
9. S. S. Kim, H. Utsunomiya, J. A. Koski, B. M. Wu, M. J. Cima, J. Sohn, K. Mukai, L. G. Griffith, J. P. Vacanti, *Ann. Surg.* **1998**, *228 (1)*, 8.
10. T.D. Roy, J.L. Simon, J.L. Ricci, E.D. Rekow, P. van Thompson, J.R. Parsons, *J Biomed Mater Res* **2003**, *67A*, 1228.
11. C. X. F. Lam, X. M. Mo, S. H. Teoh, D. W. Hutmacher, *Materials Science and Engineering* **2002**, *C 20 (1 – 2)*, 49.
12. S.–J. J. Lee, E. Sachs, M. Cima, *Rapid Prototyping Journal* **1995**, *1 (4)*, 24.
13. H. Seitz, W. Rieder, S. H. Irsen, B. Leukers, C. Tille, *J Biomed Mater Res Part B: Appl Biomater* **2005**, *74B*, 782.
14. T.F. Slater, B. Sawyer, U. Straeuli, *Biochimica Biophysica Acta* **1963**, *77*, 383.
15. T. Mosmann, *Journal of Immunological Methods* **1983**, *65*, 55.
16. Y. Maekawa, K. Yagi, A. Nonomura, R. Kuraoku, E. Nishiura, E. Uchibori, K. Takeuchi, *Thrombosis Resarch* **2003**, *109*, 309.
17. R.M. Leven, A.S. Virdi, D. R. Sumner, *J Biomed Mater Res* **2004**, *70A*, 391.
18. V. Olivier, N. Faucheux, P. Hardouin, review, Drug Discovery Today, 9(18) **2004**, 803.
19. Society of Free Radical Reseach (Australia) Newsletter September 2002, Conference details of research activities of Michael Berridge.
20. M.V. Berridge, A.S. Tan, *Protoplasma* **1998**, *205*, 74.
21. A.S. Tan, M.V. Berridge, *Journal of Immunological Methods* **2000**, *238*, 59.
22. P.M. Herst, A.S. Tan, D.J. Scarlett, M.V. Berridge, *Biochimica and Biophysica Acta* **2004**, *1657*, 79.
23. D. Wendt, A. Marsano, M. Jakob, M. Heberer, I. Martin, *Biotechnol Bioeng* **2003**, *84*, 205.
24. J. van den Dolder, G. N. Bancroft, V. I. Sikavitsas, P. H. M. Spauwen, J. A. Jansen, A. G. Mikos, *J Biomed Mater Res* **2002**, *64A*, 235.
25. G. N. Bankcroft, M. D. V. I. Sikavitsas, A. G. Mikos, *Tissue Engineering* **2003**, *9*, 549.

Corresponding author: Dr. Leukers, Research center caesar, Ludwig-Erhard-Allee 2, 53175 Bonn, E-mail: leukers@caesar.de

Received in final form: October 21, 2005 [T 968]